

# Gain-enhanced and Mechanical Reconfigurable Slot Antenna with Metasurface

Xueyan Song, Ang Dong, Xuping Li, Yunqi Zhang, Haoyuan Lin, Yapeng Li, and Hailong Yang

School of Electronic Engineering

Xi'an University of Posts & Telecommunications, Xi'an, 710121, China

xysong65@xupt.edu.cn, 1361580350@qq.com, lixuping@163.com, johnny\_5@126.com

2806198782@qq.com, liyapengedu@163.com, yanghl68@163.com

**Abstract** – A novel wideband slot antenna with metasurface is presented. In order to achieve broadband, high-gain, and mechanical reconfigurable performance, a metasurface is adopted and combined with a new-type planar slot antenna. The antenna and metasurface are designed on F4B substrate, and the overall dimension of the antenna is  $1.48\lambda_0 \times 1.48\lambda_0 \times 0.2\lambda_0$  ( $\lambda_0$  is the free space wavelength at center frequency). Different from the traditional square metasurface, a structure with different properties in the  $x$  and  $y$  directions is utilized in the proposed antenna, which can be reconstructed by adjusting the relative position between the slot antenna and the metasurface. By introducing the metasurface, the maximum gain of the whole antenna is improved. The antenna works in two states with respect to the two locations of the metasurface. The impedance bandwidth of the proposed antenna in state A is from 5.49 to 9.40 GHz (52.5%), and the impedance bandwidth of the proposed antenna in state B is from 5.83 to 6.01 GHz (3%) and 7.05 to 9.62 GHz (30.8%). The gain of the whole antenna in both states is higher than that of the original slot antenna (without metasurface), and the maximum gain is 9.1 dBi.

**Index Terms** – Metasurface, reconfigurable performance, slot antenna, wideband.

## I. INTRODUCTION

Antennas with wideband, high-gain, and programmable properties have attracted significant attention from academics in the field of wireless communication due to the growing demand of wireless communication systems [1], [2]. Due to their ability to manipulate electromagnetic waves, metasurfaces have been designed to obtain various performances in antennas [3], [4]. Usually, the structure of reconfigurable antennas can be mechanical or electrical. Electrical reconfigurable antennas are popular, and their states can be switched by

PIN-diode switches [5], [6]. However, there are some problems to be solved. For example, the addition of electronic components may affect the performance of the antenna. The operation of the antenna depends on the reliability of the electronic components and the DC power supply [7].

The metasurface has been demonstrated in the literatures [8–12]. When combined with metasurface, the antenna can achieve reconfigurable performance. In [8], a polarization and frequency-reconfigurable antenna with metasurface was proposed to reconfigure the performance of the antenna by changing the relative positions of the metasurface and antenna layer. The antenna proposed in [8] can achieve a bandwidth of 8 to 11.2 GHz (33.33%). In [9], two layers of metasurfaces are loaded above the slot antenna, and the frequency reconfigurable characteristic is achieved by rotating the top metasurface with respect to the center of the slot antenna. The operating frequency band ranges from 2.55 to 3.45 GHz (28%). And the gain curve of the antenna ranges from 5.3 dBi to 8.3 dBi. Because it does not require additional biasing circuits or switches, the physical rotation technique is attractive, which is adopted in this paper to achieve radiation pattern and impedance bandwidth reconfiguration. Therefore, the state of the proposed design in this paper can be freely switched in the communication system to achieve interference immunity. Methods to improve the overall antenna gain by incorporating metasurfaces have been used extensively, such as using the metasurface as a reflector [10],[11] and using the metasurface as a secondary radiation source to modulate the beam [12]. Nevertheless, the bandwidth and the gain of the designed antenna needs to be further improved.

In this letter, an antenna that can achieve mechanical reconfigurability, gain enhancement, and wideband is proposed. The antenna consists of a metasurface and a slot antenna, which are connected by a nylon column. In order to enhance the gain, a metasurface structure is utilized under a broadband slot antenna. The metasurface

is composed of 66 units to achieve different responses to incident waves in  $x$  and  $y$  directions. To achieve broadband characteristic, some new structures such as gradual feeder line are introduced in the presented slot antenna. The proposed antenna operates in two radiation states by mechanical rotation, and gain of the proposed antenna can be enhanced in both states compared with the original slot antenna (without metasurface). The antenna in state A provides fractional bandwidths of 52.5% at 7.45 GHz, and the antenna in state B provides fractional bandwidths of 3% at 5.92 GHz and 30.8% at 8.34 GHz. And the maximum gain of proposed antenna can reach 9.1 dBi. All in all, the proposed antenna can achieve broadband, high-gain and mechanically reconfigurable characteristics.

## II. ANTENNA DESIGN

### A. Antenna configuration

The proposed antenna consists of a new slot antenna and a metasurface, as shown in Fig. 1. The antenna and the metasurface are printed on a 1 mm substrate with

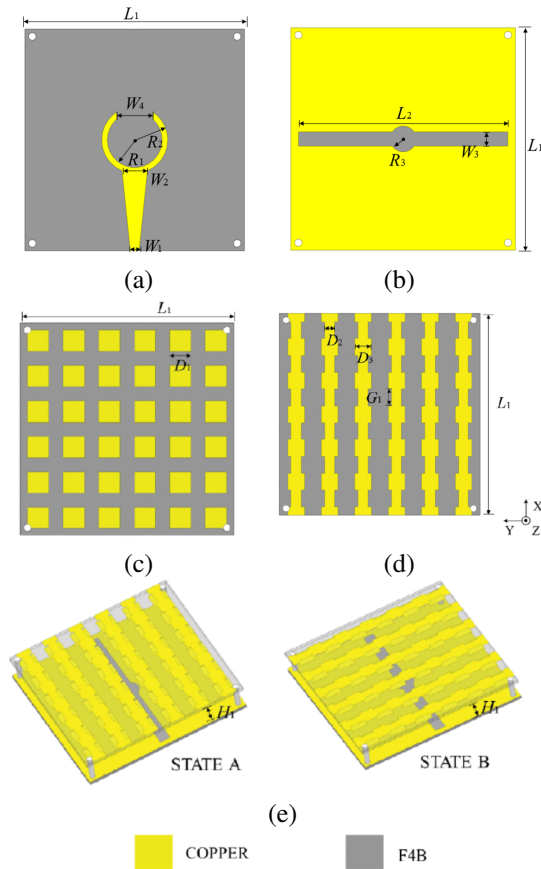


Fig. 1. (a) Feeder line of slot antenna, (b) surface of slot antenna, (c) bottom view, (d) top view of the metasurface, and (e) 3D geometry of proposed structure in states A and B.

Table 1: Dimensions of the proposed antenna (unit: mm)

Parameter	Value	Parameter	Value
$L_1$	60	$L_2$	56
$R_1$	7.5	$R_2$	9
$R_3$	3.5	$W_1$	2.4
$W_2$	6.95	$W_3$	1.9
$W_4$	10	$D_1$	6
$D_2$	3	$D_3$	5
$G_1$	5	$H_1$	8

a relative permittivity of 2.2 and loss tangent of 0.001. The antenna is on the top layer, and the metasurface is on the bottom layer. In order to improve the impedance bandwidth of the slot antenna, a new gradual feeder line, which splits at the end into a two-part circular arc and circular slot are designed, as shown in Figs. 1 (a) and (b). The metasurface is composed of  $6 \times 6$  two-layer patch units, which are etched on the both sides of one substrate. The top patch layer is arranged by an inverted H-shaped patch unit in  $x$  and  $y$  directions and the bottom layer consists of a square patch. The units are designed as shown in Figs. 1 (c) and (d). By rotating the metasurface around the center with respect to the slot antenna, the reconfigurable characteristic of the proposed antenna can be achieved. The detailed operation of mechanical reconfiguration is achieved by manually adjusting the four nylon columns on the four corners of the substrates. When the four columns are unscrewed, the metasurface can be manually rotated by 90 degrees around the  $z$ -axis along the center, and then installed under the antenna, bringing in the switching between two states. The structure of the proposed antenna in two states is shown in Fig. 1 (e). The dimensions of the antenna are shown in Table 1.

### B. Working mechanism

The characteristics of the proposed slot antenna and metasurface are simulated by using ANSYS HFSS. In order to obtain broadband characteristics of the slot antenna, the design of the feeder line is especially important. The impedance characteristics of the slot antenna can be greatly improved by the design of the tapering structure and the open ring. Therefore, of all the parameters,  $R_1$  and  $W_1$  make great contributions to the characteristics of the slot antenna. Figure 2 depicts the simulated  $S_{11}$  of the proposed antenna with different values of  $R_1$  and  $W_1$ . From Fig. 2 (a), it can be seen that when  $R_1$  decreases, the resonance characteristics of the low frequency band become worse, when  $R_1$  increases, mainly the resonance characteristics of the high frequency part become worse. when  $R_1 = 7.5$  mm, the impedance bandwidth is the best, From Fig. 2 (b), it can be seen that when  $W_1$  changes, there will be two frequency points

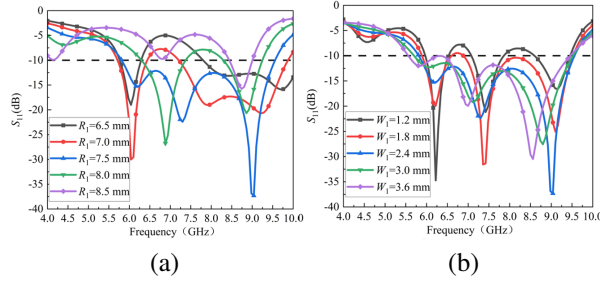


Fig. 2. Simulated  $S_{11}$  of the proposed slot antenna with different values of the main parameters including (a)  $R_1$ , and (b)  $W_1$ .

where the resonance performance becomes worse. When  $W_1 = 1.8$  mm, the impedance bandwidth is optimal. To obtain good matching property, it reaches a compromise to choose the value  $R_1$  as 7.5 mm and  $W_1$  as 2.4 mm.

As mentioned above, the reconfigurability of the antenna results from the units of the metasurface. When the metasurface and the antenna are in two different relative positions, the metasurface can achieve transmission and reflection performance, respectively. The units of the metasurface are shown in Figs. 3 (a) and (b). In order to investigate properties of the metasurface, the unit cell is simulated by the simulation software ANSYS HFSS, and the simulation model is shown in Fig. 3 (c). The unit is imposed by the Master-Slaver boundary conditions and excited by the Floquet ports. With this electromagnetic simulation method, the response characteristics

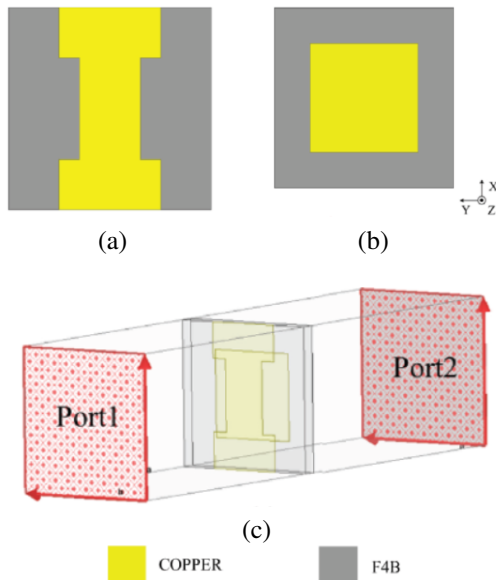


Fig. 3. (a) Top view of the unit cell, (b) bottom view of the unit cell and (c) the simulation model of the proposed unit cell of the metasurface.

of the metasurface with infinitely large dimensions can be simulated and thus save computational resources.

For different incident waves in  $x$ -polarized and  $y$ -polarized directions, the metasurface works in a different state. When the incident wave is  $x$ -polarized, the metasurface is reflective, which is defined as state A; and when the incident wave is  $y$ -polarized, the metasurface is transmissive, which is defined as state B. When in state A, electromagnetic energy is reflected from the metasurface and superimposed, which contributes to the improvement of the maximum gain. And when in state B, the aperture of the antenna is increased by the addition of a metasurface, which narrows the beam and raises maximum gain.

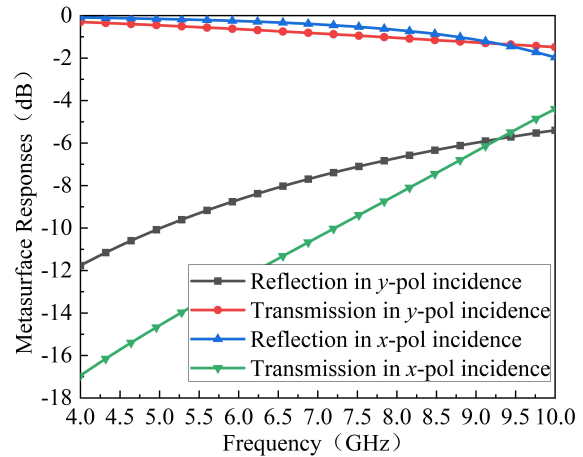


Fig. 4. Simulated reflection and transmission coefficients of metasurface.

The response of the metasurface from the incident  $x$ -polarized wave and  $y$ -polarized wave is shown in Fig. 4. It can be seen from the blue curve in Fig. 4, when the incident electromagnetic wave is  $x$ -polarized, the metasurface reflects the majority of the energy. From the red curve in Fig. 4, it can be obtained that the metasurface transmits most of the energy when the incident electromagnetic wave is  $y$ -polarized. Due to the different performances of the metasurface in two states, the proposed antenna in this work can achieve various characteristics.

In order to investigate the influence of the metasurface on the original slot antenna, the proposed combined antenna at 6.5 GHz in two states is taken as an example. And Fig. 5 depicts the electric field intensity distribution of the antenna in both states, from which it can be determined that the electric field intensity distribution the both sides of the slot and terminal feeder line are different. That is because the addition of the metasurface changes the electromagnetic environment around the slot antenna. When operating in state A, the slot antenna

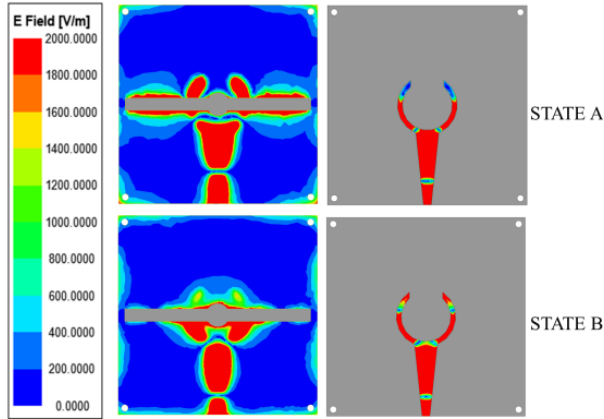


Fig. 5. Electric field distributions in states A and B at 6.5 GHz.

around the electromagnetic energy is scarcely affected because the metasurface is transmissive, bringing in the similar frequency response between the whole antenna in state A and the original slot antenna (without metasurface). In state B, the metasurface reflects the energy initially radiated in the  $+z$  direction. The reflected energy is then excited again on the terminal feeder line of the slot antenna, which results in the difference in reflection coefficient between the whole antenna in state B and the original slot antenna at 6.5 GHz.

### III. SIMULATED RESULTS

The simulated  $S_{11}$  and radiation efficiency of the original proposed slot antenna (without metasurface) and the whole antenna in states A and B are shown in Fig. 6. It can be seen that the original slot antenna operates in the band between 5.81 GHz and 9.56 GHz (48.8%). The bandwidth of the whole antenna in state A is from 5.49

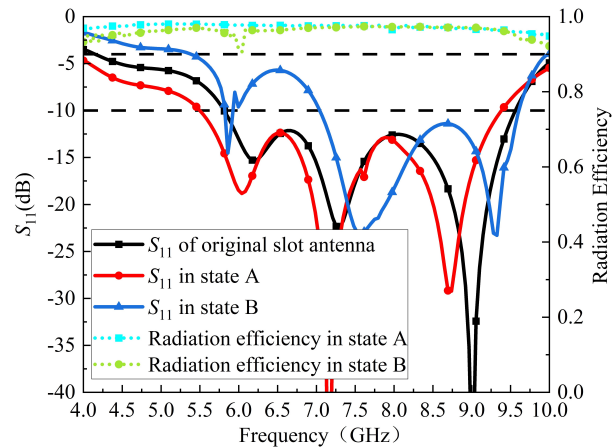


Fig. 6. Simulated  $S_{11}$  and radiation efficiency of the proposed original slot antenna and the slot antenna with metasurface in two states.

GHz to 9.40 GHz (52.5%). The bandwidth of the whole antenna in state B is 5.83 GHz to 6.01 GHz (3.0%) and 7.05 GHz to 9.62 GHz (30.8%). And the radiation efficiency of the proposed antenna is greater than 90% in two states.

Figure 7 depicts the radiation patterns in  $xoz$  and  $yoz$  plane of the original slot antenna, and the whole antenna in state A and state B at 6 GHz, 7.5 GHz, and 9 GHz. As shown in Fig. 7, the maximum gain of the antenna in both state A and state B is higher than that of the original slot antenna. Moreover, it can also be seen that the addition of the metasurface makes the original slot antenna generate two radiation patterns, which brings in reconfigurable achievement. Table 2 demonstrates the increase in maximum gain of the proposed antenna at the three frequency points. It can be found that, with the metasurface, the proposed slot antenna can achieve significantly

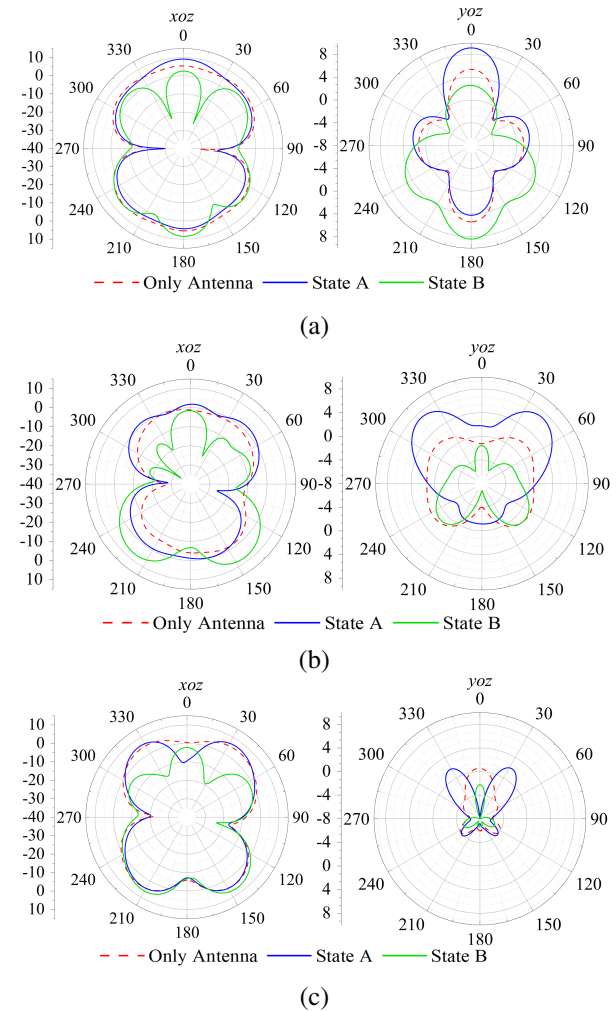


Fig. 7. The simulated radiation patterns of the proposed slot antenna with and without metasurface at (a) 6 GHz, (b) 7.5 GHz, and (c) 9 GHz.

Table 2: Gain enhancement effect (unit: dBi)

Frequency (GHz)	Only Antenna	State A	State B	State A Enhance	State B Enhance
6	5.6	9.1	8.4	3.5	2.8
7.5	3.4	7.1	7.7	3.7	4.3
9	5.8	6.7	8.1	0.9	2.3

more gain improvement than the original slot antenna. The maximum gain of the slot antenna with metasurface can reach 9.1 dBi.

#### IV. EXPERIMENTAL RESULTS

To verify the antenna performance, a prototype of the same size as in Table 1 is fabricated and measured. The specific appearance is shown in Fig. 8. For easy switching between state A and state B, four nylon columns are fixed to connect the antenna and the metasurface. The reflection coefficient is measured by Keysight E5063A network analyzer.

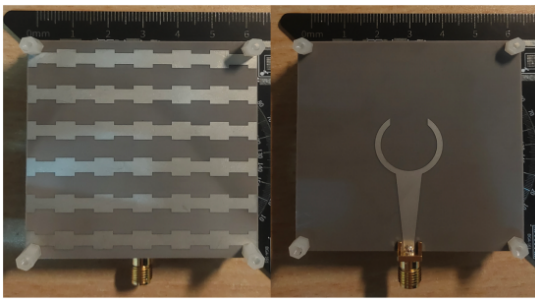


Fig. 8. Front and back sides of the prototype.

The simulated and measured  $S_{11}$  in state A and state B are depicted in Fig. 9. It can be seen that the measured results are in good accordance with the simulated ones except for small deviations in operating frequencies, which are mainly due to fabrication and experimental tolerances. The operating bandwidth of the antenna in state A is from 5.41 GHz to 9.55 GHz (55.35%). The operating band of the antenna in state B ranges from 5.95 GHz to 6.13 GHz (3%) and from 7.03 GHz to 9.87 GHz (33.6%). The radiation patterns are measured in the microwave lab. The simulated and measured radiation patterns of the proposed antenna in state A and B in  $xoz$  and  $yoz$  plane at 8 GHz are shown in Fig. 10. The proposed antenna exhibits different radiation characteristics in different states and realizes the reconfigurable characteristics in the radiation patterns. In the  $xoz$  plane, the cross-polarization is less than -30 dB. The cross-polarization level in the  $yoz$  plane is small in the direction of maximum radiation and does not affect communication. The little difference between the measured and the

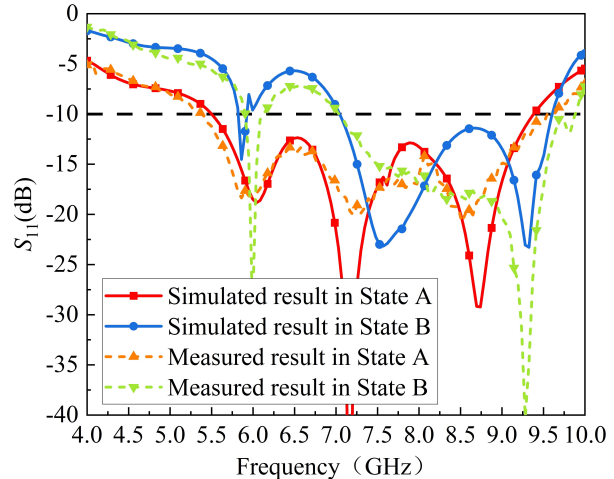
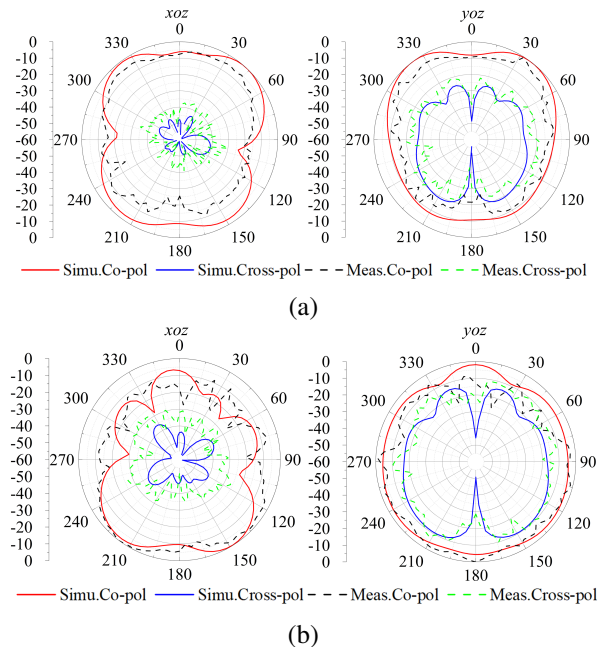
Fig. 9. Simulated and measured  $S_{11}$  of the proposed antenna in state A and state B.

Fig. 10. Simulated and measured radiation patterns of the proposed antenna at 8 GHz in (a) state A and (b) state B.

simulated results is mainly due to the measure environment and manufacturing errors.

The performances of the proposed antenna compared with that of antennas are illustrated by Table 3 in references. Compared with [4], [7], and [9–11], the proposed antenna has a wider bandwidth and high gain. Compared with [8], the dimension of the proposed antenna is smaller and the bandwidth is wider. In conclusion, the proposed antenna can achieve broadband, high-gain, and reconfigurable characteristics.

Table 3: Comparison of the proposed antenna and references

References	Bandwidth (%)	Gain (dBi)	Overall size ( $\lambda 0$ )	Whether Reconfigurable
[4]	23.6	8.1	$0.78 \times 0.78 \times 0.038$	no
[7]	14.6	5	$0.67 \times 0.67 \times 0.05$	yes
[8]	33.33	16.5	$2.56 \times 2.56 \times 0.93$	yes
[9]	28	8.3	$1 \times 1 \times 0.07$	yes
[10]	40	9.9	$1.2 \times 1.2 \times 0.12$	no
[11]	43.1	6.12	$0.348 \times 0.348 \times 0.07$	No
This work	52.5	9.1	$1.48 \times 1.48 \times 0.2$	yes

## V. CONCLUSION

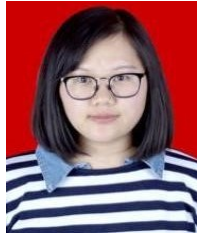
In this paper, a reconfigurable, high-gain, and wide-band slot antenna with metasurface is designed and fabricated, and two radiation states can be realized by physically rotating the metasurface. The impedance bandwidth of the proposed antenna in state A is from 5.49 GHz to 9.40 GHz (52.5%), and the impedance bandwidth of the proposed antenna in state B is from 5.83 GHz to 6.01 GHz (3%) and from 7.05 GHz to 9.62 GHz (30.8%), and the maximum gain reaches 9.1 dBi. The measured results agree well with the simulated ones, which validates that the antenna has the advantages of large bandwidth, high gain, and reconfigurable performance. Therefore, the proposed antenna can be utilized in C and X bands for high-capacity microwave communication, such as satellite communication and medical service.

## ACKNOWLEDGMENT

This work was supported by the Natural Science Basic Research Program of Shaanxi (Program Nos. 2022JQ-699, 2022JQ-633, and 2021JQ-710) and the Key Research and Development Program of Shaanxi (Program No. 2021GY-049).

## REFERENCES

- [1] H. Li, G. Wang, X. Gao, J. Liang, and H. Hou, "A novel metasurface for dual-mode and dual-band flat high-gain antenna application," *IEEE Transactions on Antennas and Propagation*, vol. 66, pp. 3706-3711, July 2018.
- [2] B. Heydari, A. Afzali, and H. R. Goodarzi, "A new ultra-wideband omnidirectional antenna [antenna designer's notebook]," *IEEE Antennas and Propagation Magazine*, vol. 51, no. 4, pp. 124-130, Aug. 2009.
- [3] D. Chen, W. Yang, Q. Xue, and W. Che, "Miniaturized wideband planar antenna using interembedded metasurface structure," *IEEE Transactions on Antennas and Propagation*, vol. 69, no. 5, pp. 3021-3026, May 2021.
- [4] J. Zhu, G. Zhang, Z. Li, Z. Che, J. Yue, Y. Feng, Q. Zhang, and R. Qiu, "A high-gain, low-profile filtering antenna based on a novel metasurface," *Applied Computational Electromagnetics (ACES) Journal*, vol. 37, no. 11, pp. 1153-1161, Apr. 2023.
- [5] Y. Liu, W. Zhang, Y. Jia, and A. Wu, "Low RCS antenna array with reconfigurable scattering patterns based on digital antenna units," *IEEE Transactions on Antennas and Propagation*, vol. 69, no. 1, pp. 572-577, Jan. 2021.
- [6] M. Shirazi, J. Huang, T. Li, and X. Gong, "A switchable-frequency slot-ring antenna element for designing a reconfigurable array," *IEEE Antennas and Wireless Propagation Letters*, vol. 17, no. 2, pp. 229-233, Feb. 2018.
- [7] H. L. Zhu, X. H. Liu, S. W. Cheung, and T. I. Yuk, "Frequency-reconfigurable antenna using metasurface," *IEEE Transactions on Antennas and Propagation*, vol. 62, no. 1, pp. 80-85, Jan. 2014.
- [8] C. Ni, M. S. Chen, Z. X. Zhang, and X. L. Wu, "Design of frequency-and polarization-reconfigurable antenna based on the polarization conversion metasurface," *IEEE Antennas and Wireless Propagation Letters*, vol. 17, no. 1, pp. 78-81, Jan. 2018.
- [9] B. Majumder, K. Krishnamoorthy, J. Mukherjee, and K. P. Ray, "Frequency-reconfigurable slot antenna enabled by thin anisotropic double layer metasurfaces," *IEEE Transactions on Antennas and Propagation*, vol. 64, no. 4, pp. 1218-1225, Apr. 2016.
- [10] Z. Jiang, Z. Wang, L. Nie, X. Zhao, and S. Huang, "A low-profile ultrawideband slotted dipole antenna based on artificial magnetic conductor," *IEEE Antennas and Wireless Propagation Letters*, vol. 21, no. 4, pp. 671-675, Apr. 2022.
- [11] D. Feng, H. Zhai, L. Xi, S. Yang, K. Zhang, and D. Yang, "A broadband low-profile circular-polarized antenna on an AMC reflector," *IEEE Antennas and Wireless Propagation Letters*, vol. 16, pp. 2840-2843, 2017.
- [12] D. Chen, Q. Xue, W. Yang, K.-S. Chin, H. Jin, and W. Che, "A compact wideband low-profile metasurface antenna loaded with patch-via-wall structure," *IEEE Antennas and Wireless Propagation Letters*, vol. 22, no. 1, pp. 179-183, Jan. 2023.



**Xueyan Song** was born in Henan Province, China, 1989. She received the B.E. degree in electronic and information engineering from Xidian University, Xi'an, China, in 2012. She received the Ph.D. degree from Xidian University, Xi'an, China, in 2018. She joined the School of Electronic Engineering, Xi'an University of Posts and Telecommunications in 2018. Her research interests include artificial magnetic conductors, low RCS antennas, low-profile antennas, frequency selective surfaces, and reflector antennas.



**Ang Dong** was born in Hebei, China, in 1999. He is currently pursuing a Master of Engineering degree in the School of Electronic Engineering, Xi'an University of Posts and Telecommunications. His current research interests include metasurface, microstrip antennas.



**Xuping Li** was born in Xi'an, Shanxi, China in 1981. He received the Ph.D. degree in electromagnetic field and microwave from the Xidian University, Xi'an, China in 2015. In January 2019, he was transferred to Xi'an University of Posts and Telecommunications as the leader of the phased array antenna technology research team. The principal focus of his research program is the development of phased array antennas.



**Yunqi Zhang** was born in BaoTou, Inner Mongolia, China, in 1986. He received the Ph.D. degree from Xidian University, Xi'an, China in 2015. He is currently working in the Xi'an University of Posts & Telecommunications. His research interests include GPS antennas, CP antennas, omnidirectional antennas, and antenna array designs.



**Haoyuan Lin** was born in Shandong, China, in 2003. He is currently pursuing a B.E. degree in the school of Electronic Engineering from Xian University of Posts and Telecommunications. His current research interests include circuits, microwave, antennas.



**Hailong Yang** received the B.S. in communicating engineering from Heze University, Heze, China, in 2012, M.S. and Ph.D. degrees in communicating engineering from Xi'an University of Technology, Xi'an, China, in 2015 and 2019. He joined the faculty of Electronic Engineering Department, Xi'an University of Posts&Telecommunications, in 2019. His research interests include wave propagation and antenna design.



**Yapeng Li** received the Doctor's degree from Xidian University in 2020. He is currently an associate professor with the School of Electric Engineering, Xi'an University of Post and Telecommunications. His research interests include filtering antennas, wideband antennas, dual-polarized antennas and circular polarized antennas.